Solvent dependent folding of an amphiphilic polyaramid

Angélique Molliet,[1] Samantha Doninelli,[1] Linda Hong, [1] Bettina Tran,[1] Meron Debas,[1] Stefan Salentinig, [1]* Andreas F.M. Kilbinger[1]*

Tommaso Casalini[2,3]*

1 Department of Chemistry, University of Fribourg, Chemin du Musée 9, CH-1700 Fribourg, Switzerland.

2 Department of Chemistry and Applied Bioscience, Institute for Chemical and Bioengineering, ETH Zurich, Vladimir-Prelog-Weg 1-5/10, Zürich, 8093, Switzerland.

3 Polymer Engineering Laboratory, Institute for Mechanical Engineering and Materials Technology, University of Applied Sciences and Arts of Southern Switzerland (SUPSI), Via la Santa 1, Lugano, 6962, Switzerland.

aromatic amide foldamers, aramid, helix, amphiphilic polymers, small angle x-ray scattering, molecular dynamics simulations, metadynamics

ABSTRACT: A series of synthetic alternating and amphiphilic aromatic amide polymers were synthesized by step growth polymerization. Alternating *meta* and *para*-linkages were introduced to force the polymer chain into a helical shape in the highly polar solvent water. The polymers were analyzed by ^{1}H-NMR spectroscopy and SEC in polar aprotic solvents such as DMSO and DMF. However, the polymers also showed good solubility in water. ^{1}H-NMR spectroscopy, small angle X-ray scattering and dynamic light scattering provided clear evidence of polymer folding in water but not DMF. We employed parallel tempering metadynamics in the well-tempered ensemble (PTMetaD-WTE) to simulate the free energy surfaces of an analogous model polymer in DMF and water. The simulations gave a molecular model of an unfolded structure in DMF and a helically folded tubular structure in water.

Introduction

For many decades, helical foldamers and hollow polymeric tubes have been extensively developed due to their potential applications in molecular recognition and transmembrane transport. Aromatic polyamides are the most studied structures due to their rigid and conformationally predictable backbones and convenient synthesis. In 1994, Hamilton and co-workers were the first to report the helical folding of an amide-based pentamer consisting of an alternation of anthranilic acid with 2,6-pyridinedicarboxylic acid.[1,2] This oligomer was fully rigidified and stabilized by six intramolecular hydrogen-bonds and additional π-π stacking. New scaffolds with cavities of tunable sizes emerged: Gong and *al.* reported the formation of helical oligomers based on 5-amino-2,4-alkoxybenzoic acid.[3,4,5,6,7] Intramolecular three-center H-bonds formed between the amide N-H and the alkoxy group. Additional aromatic stacking led to a locked conformation with a hydrophilic interior cavity diameter of around 10 Å. The inside of this electrostatically negative cavity was reported to trap guest molecules such as the octylguanidinium cation. Moreover, by incorporating building blocks containing *p*-substituents, the curvature of the oligomer could be modified to reach an inner diameter of > 30 Å. Huc and co-workers developed stable helical oligomers based on 8-amino-2-quinolinecarboxylic acid.[8,9,10,11,12] They prepared long oligomers comprising up to 34 repeat units, corresponding to a 13-turn helix of 5.1 nm in length. It could also be demonstrated that those helices could bind Cu^{II} ions in their cavity through amide deprotonation, thus forming a Cu^{II} wire. By brominating their monomer, Huc and coworkers could simplify the purification steps and reach even longer foldamers with 96 quinoline repeat units.[13,14] The Li group demonstrated that other proton acceptors, including aromatic fluorides, could also be used to design oligoaramid foldamers.[15,16] They synthesized heptamers based on derivatives of 2-fluoroisophtalic acid and 2-fluorobenzene-1,3-diamine. The intramolecular interaction between the fluorine atom and the amide proton led to a helical conformation. This created a polar internal cavity possessing an inner diameter of around 6.5 Å capable of binding dialkylammonium ions. Over the years, a broad diversity and combination of building blocks able to form helical amide foldamers were designed.[3,4,5,6,7,17,18,12,15,16] The synthesis of long oligomers consisting of many turns often involves demanding and fastidious iterative condensation steps, which are hardly compatible with achieving long sequences. Indeed, the steric hindrance resulting from the folding of the oligomer during the reaction and the low reactivity of some aromatic amines are often responsible for the low yield obtained and the long reaction time needed.[14] Therefore, to get longer helices in one pot, polymerization techniques were explored. Monomers based on well-known H-bond driven helical foldamers were investigated.[19,20,21,22,23] Gong, Zhu, and co-workers tried to extend the length of their three-centered H-bond oligomers by condensing the corresponding monomeric diacid chlorides and diamines.[20] Unfortunately, instead of a polymer, they observed the formation of macrocycles due to the exceedingly stable intramolecular H-bond pattern. To obtain high molecular weight polymers, they replaced their diamine monomer with a slightly more flexible one, getting an 18-turn helical polymer. Guan and Li *et al.* used the Yamazaki-Higashi polycondensation method for their 3-amino-2-methoxy-5-

methylbenzoic acid monomer and obtained a partially demethylated polymer.[21] By adding a chiral inducer after complete re-methylation, they observed a signal in circular dichroism (CD) indicative of helical structures. Zeng et al. reported using $POCl_3$ as a coupling agent for polymerizing their previously reported pyridine-based aromatic foldamers.[22] With this method, they could synthesize nanotubes of 2.8 nm in length capable of selectively transporting protons and water.[23] These helical polymers are driven by intramolecular H-bond interactions, which make the polycondensation difficult owing to the steric hindrance resulting from the folding.

Another driving force, the solvophobic effect, can be used as an alternative as it induces the folding only in certain solvents, typically water or highly polar solvents. [24,25] However, until now, only a few reports used this effect to cause the folding of aromatic polyamides. Yokozawa and *al.* reported that the folding of poly(naphthalenecarboximide)s bearing a tri(ethylene glycol) side chain was enhanced in water due to the solvation of the hydrophilic chain and the intramolecular self-association of the hydrophobic naphthalene rings.[26,27] Li, Wang and co-workers developed water soluble polymers based on benzene-naphthalene and benzene bipyridine alternating monomers.[28,29,30] They demonstrated that the high hydrophobicity of the naphthalene ring combined with the H-bond capacity of amide groups was generating a helical structure not only in water but also in less polar solvents due to the intramolecular H-bonding across layers. The initial helical conformation could be inverted into another helical state when using bipyridine as an alternating monomer and combining it with Ni^+ ions.

Herein, we report the synthesis and water-induced folding of an aromatic polyamide prepared from alternating a hydrophobic monomer bearing an ethylhexyl side chain and hydrophilic monomers carrying a basic tertiary amine as a side group. This polymer possesses an inner cavity of 2.5 nm and requires 10 monomer units for one turn.

Results and Discussion

Synthesis. The synthesis of monomers and polymers is shown in Scheme 1. The synthesis of hydrophilic monomers **2a** and **2b** started with the one-pot mild acylation of 3,5-dinitrobenzoic acid using Ghosez's reagent followed by a reaction with 2-dimethylamino-ethanol or *N,N*-dimethylethylendiamin to give **1a**, respectively **1b** in good yields (Scheme 1). Reduction of the nitro groups with Pd/C and hydrogen led to the final hydrophilic monomers **2a** and **2b**.

The synthesis of the hydrophobic monomer began with a reductive amination of dimethyl aminoterephthalate with racemic 2-ethylhexanal, followed by a substitution reaction with methyl iodide to give compound **4**. Finally, hydrolysis of **4** with KOH gave the final product **5** in 92 % overall yield.

The Yamazaki-Higashi polycondensation method was used to avoid the formation of HCl during the polymerization.[31,32] This reaction involves the formation of a complex between pyridine and triphenyl phosphite, leading to an acyloxy *N*-phosphonium salt of pyridine. The successive aminolysis results in the construction of the polymer. The polymerization is based on condensing a linear hydrophobic diacid monomer (**5**) with a meta-substituted hydrophilic diamine (**2a**, **2b**). In neutral (pH=7) water, the hydrophilic dimethylamino groups (pKa ca. 9.2, dimethylmonoethanolamine was used as a reference[33]) are expected to be fully protonated and would, therefore, interact well with the solvent.

On the other hand, the hydrophobic chains would minimize the contact with water by forming a helical structure, thus creating an inner hydrophobic cavity (Scheme 2) owing to the hydrophobic effect. Monomer **5** was, therefore, combined with either monomer **2a** or **2b** to form polymers **6a** and **6b** (GPC_{DMF}: Mn= 14200 Da, Đ = 1.46), respectively. Two different reaction times during the polymerization of **2a** with **5** allowed us to obtain two different polymers, **6a-1** (GPC_{DMF}: Mn=13900 Da, Đ =2.3) and **6a-2** (GPC_{DMF}: Mn=19000 Da, Đ =3.2). Despite many re-precipitations in acetone, triphenyl phosphite byproducts were still present in the polymer as shown by NMR analysis. Recycling GPC in DMF, however, allowed us to purify the samples and remove all traces of phosphite impurities. The ^1H NMR spectrum in DMSO-d_6 allowed us to observe the aromatic region of polymer **6a-2** free of byproducts (see Supporting Information S4) confirming the expected structure.

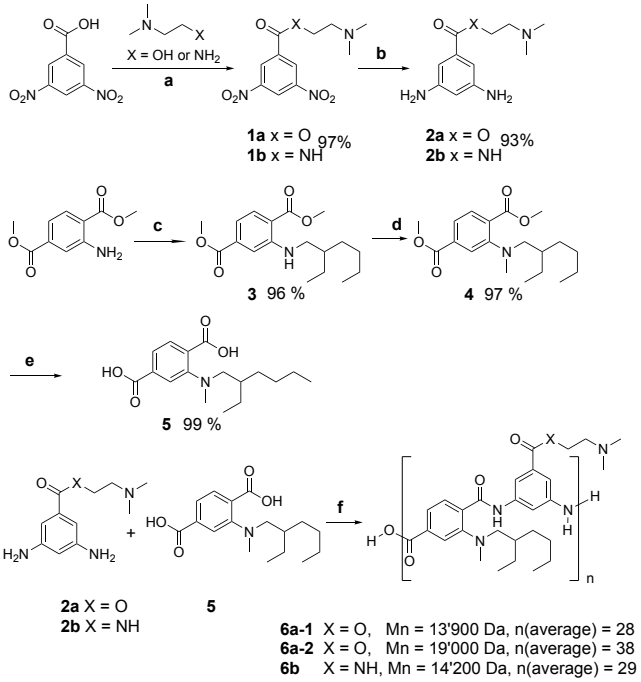

Scheme 1 Synthesis of hydrophilic (**2a**, **2b**) and hydrophobic (**5**) monomers and polymers (**6a**, **6b**). a) 1-Chlor-*N,N*,2-trimethyl-1-propenylamin (Ghosez' reagent), dichloromethane, rt, 12h b)Pd/C, H_2, 50 bar, ethylacetate, 50°C, 4d c) *rac*-2-ethylhexyanal, sodium triacetoxyborohydride, acetic acid, dichloromethane, rt. 12h d) sodium hydride, methyl idodide, dimethylformamide, rt.12h e) potassium hydroxide, methanol:water=2:1, 24h f) triphenylphosphite, lithium chloride, pyridine, N-methylpyrrolidon, 110°C, 14d. The values *n* are rounded number average degrees of polymerization.

Conformational analysis. All polymers were soluble in DMF and DMSO as well as in water if diluted from highly concentrated DMF or DMSO (ca. 30 mg in 0.6 mL) solutions. The very high solubility of the polymers in almost pure water (95 %) may result from their helical folding, whereby the hydrophobic ethylhexyl chains are placed inside a helical cavity, shielded from the external aqueous environment (Scheme 2).

NMR analyses were performed for polymers **6a-2** and **6b** in deuterated DMF, DMSO, and water (solubilized by diluting a concentrated DMF solution, see Supporting Information Figures S1 to S9). The aromatic region could not be fully analyzed in all three cases due to triphenyl phosphite byproducts resulting from the polymerization method (see above). However, in the case of water, sharp triphenyl

phosphite peaks appeared to overlap one broad single signal. The same broadening of the peaks occurred in the aliphatic region from 0 to 2.5 ppm where the signals of the ethylhexyl side chain of monomer **5** would have been expected. In DMSO-d_6 and DMF-d_7, the signals of the hydrophobic chain are present and well resolved. In D_2O, however, those signals form only one broad peak, almost merging with the baseline. This effect is typically observed for forming aggregates with orientation dependent interactions where motional constraints lead to changes in NMR linewidths and chemical shifts resulting in peak broadening or in extreme cases complete NMR silence. We believe this is yet another indication of a probable helical folding of the polymer in water (see Supporting Information S5-S6 and S8-S9).

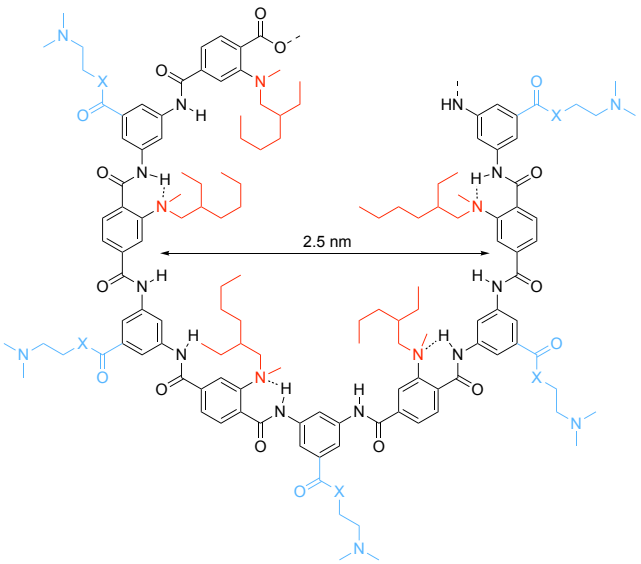

Scheme 2 Proposed model of the helical structure adopted by the polymers in water. The hydrophilic chains (in blue) are protonated and situated outside a helix where they can interact with the surrounding solvent (water). On the other hand, the hydrophobic chains (in red) orient inside the cavity, forming a hydrophobic microenvironment. Intramolecular hydrogen bonds are proposed based on ab initio calculations (see supporting information) which are shown with dotted lines.

The polymers prepared are expected to form a 50:50 mixture of left and right-handed helices. To induce a twist-sense bias, the polymers **6a-2** and **6b**, previously dissolved in a small amount of DMF, were diluted with L-(+)-lactic acid (>= 88 %) and analyzed by CD spectroscopy. We hypothesized that lactic acid could be sufficiently polar to induce a helical folding similar to that of water. Unfortunately, no CD signal could be observed. If the polymers adopted a helical shape, the lactic acid could not induce a preferential helical bias. Assuming a large helical diameter as shown in Scheme 2, it is possible that the length scales of chirality of the assumed helix and the stereogenic center of lactic acid are simply too different to induce a strong enough bias for one of the two helicities.

Polymers **6a-2** and **6b** were then analyzed by UV-vis spectroscopy keeping a constant concentration (0.258 mg/ml, respectively 0.254 mg/ml) in different water-DMF solvent ratios (vol-vol) (98-2, 85-15, 75-25, 70-30, 60-40, 50-50, 40-60, 25-75, 15-85, 0-100). While structurally similar, the UV/vis spectra of the two polymers looked somewhat different. Polymer **6a-2** shows an absorption band at around 381 nm in pure DMF (see Figure 1 and Supporting Information S10-S11). Upon adding water up to 60 %, this band undergoes a red-shift to about 392 nm. Further increase of the water content up to 98 % gave identical spectra with a hypochromic shift from 70 % to 98 % water, typical for aromatic stacking.[24,25,30,34] For polymer **6b**, only a shoulder is present in this region (see Supporting Information S13). For **6a-2**, the spectra were identical from 60 % to 98 % water content. Moreover, both polymers possess different fluorescence spectra in water and DMF upon irradiation at 366 nm (see Supporting Information S12 and S14). Those analyses showed that the polymers changed conformation at 60 % water. The two polymers only differ in how the hydrophilic side chains are connected to the helical scaffold (ester vs. amide). However, the presence of an additional *N-H* hydrogen bond donor on the outside of the helix might lead to differently folded structures in the case of the amide (**6b**) compared to the ester (**6a-2**).

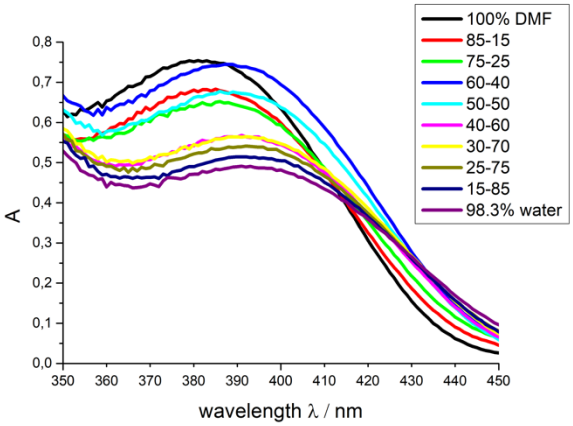

Figure 1 UV-vis spectra of polymer 6a-2 in different water-DMF ratios at a constant concentration of 0.258 mg/mL. Identical maximum absorption at around 392 nm was observable from 60% to 100% water. An hypochromic shift of the absorption maximum for 70% to 100% water solutions suggests the formation of stronger aromatic stacking upon increasing the amount of water.

It is conceivable that amide groups on the outside of the helix form hydrogen bonds between different turns of the helical fold. This could affect the helical pitch and number of monomers per turn. Similar effects have been observed for the self-assembly of macrocycles[35] and guanine-cytosine rod-like dinucleobase monomers.[36]

Small-angle X-ray scattering (SAXS) on a synchrotron source was used to investigate the folding of the polymers further. The SAXS curves of the 19k Da polymer (**6a-2**) at 2.5 mg/mL in the water-DMF mixtures (0-100, 25-75, 50-50, 75-25, 95-5, Figure S15), show the transformation of unfolded polymer aggregates into systems with structural features on the nanoscale, as indicated by the broad correlation peak in the I(q) at intermediate q values with a maximum around 0.5 nm^{-1} upon increasing the water content.

Kratky plots ($I(q)q^2$ vs. q) were used to further analyze this folding behavior of the polymers upon increasing the water content. In the Kratky plot, a folded polymer shows a broad peak at low q values, whereas, for unfolded polymers, the $I(q)q^2$ curve increases with q. The Kratky plots for **6a-2** show the transformation from unfolded polymers in DMF to (partly) folded polymers above water-DMF 50-50, with a broad peak in the $I(q)q^2$ function below q-values of 2 nm^{-1} (see **Figure S15**).

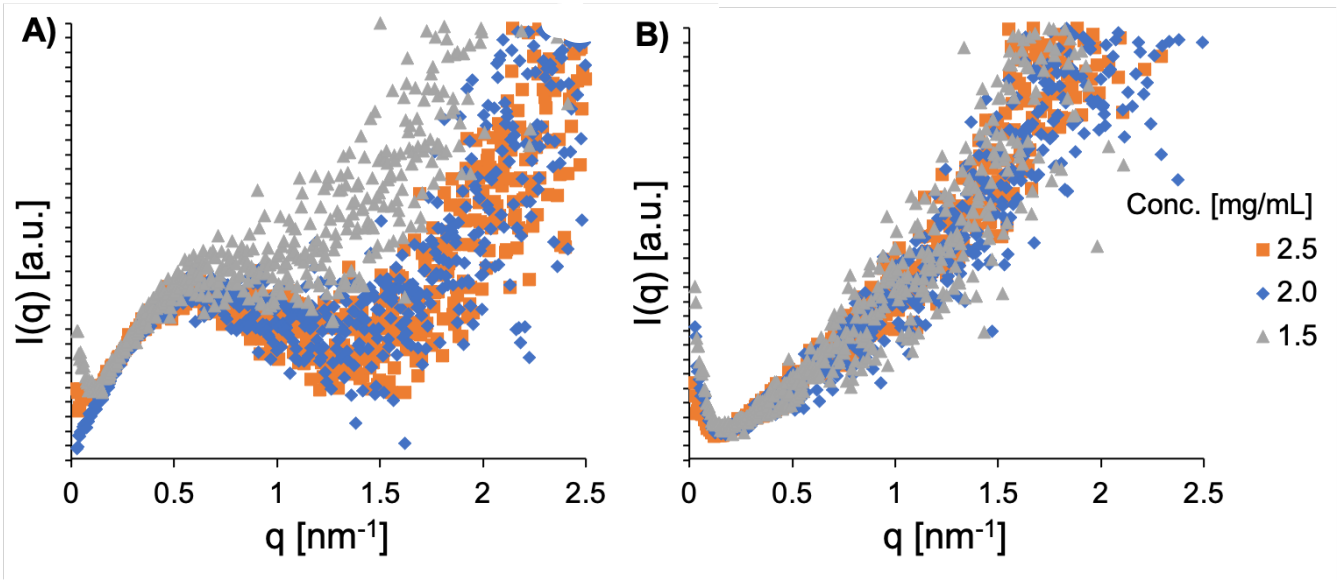

Figure 2 Kratky plot of the SAXS data **6a-2** at different concentrations in A) water-DMF 95-5, and B) DMF. The curves were scaled by the dilution factor. Partially folded polymers are observed at all concentrations in water-DMF and unfolded polymers at all DMF concentrations. The corresponding SAXS data are presented in **Figure S16**.

The Kratky plots of the SAXS curves of 6a-2 at various concentrations between 1.5 and 2.5 mg/mL in water-DMF (95-5) and DMF are shown in Figure 2, with the corresponding SAXS data in Figure S16. From Kratky analysis, the polymer is partly folded at all concentrations in water-DMF (95-5), and mostly unfolded in DMF at all concentrations. This demonstrates that the conformation of polymer 6a-2 is independent of the studied polymer concentration. The SAXS curves in Figure S16 show upturns at low q-values for all concentrations, and a transition into the overall Guinier region could not be resolved with the maximum dimension from the SAXS set-up of $\frac{\pi}{q} = 100\ nm$. Dynamic light scattering was applied to study further the shape and overall dimensions of the polymer self-assemblies.

The formation of rod-like nanoscale polymer aggregates in water was observed with (depolarized) dynamic light scattering ((D)DLS). The autocorrelation functions of the polymer **6a-2** from DLS and DDLS are shown in **Figure S17**. Reproducible autocorrelation functions could only be obtained for the 95-5 water-DMF, and the DMF samples. In DDLS, scattering only arises from optically anisotropic particles, such as rod-like polymer helices (see Methods section in the Supporting Info). The plots of the decay rate of the correlation function at different scattering angles from DLS and DDLS are presented in Figure 3. From the linear fits to the experimental Γ versus q^2 data, the translational (DLS) and rotational (DDLS) diffusion coefficients were determined. Using hydrodynamic theories of a cylinder, the length of around 328 nm and diameter of approximately 4 nm were calculated as estimates for the polymer helix; see Supporting Information for further details.

Drop cast solutions of **6a-2** (4mg/L, 5µL) onto freshly cleaved mica were also investigated by atomic force microscopy (AFM). There, fiber-like structures could be visualized with lengths above 100 nm. While the individual helices cannot account for this observation, it is conceivable that these structures represent higher aggregates composed of the end-to-end aggregation of individual helices which would be in good agreement with the data obtained for a cylindrical model in our DDLS experiments (see above).

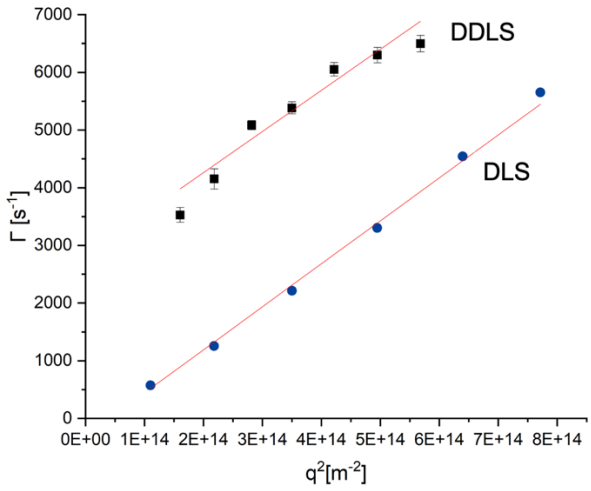

Figure 3 Decay rates versus q2 plot from DLS (in VV mode) and DDLS (in VH mode), including linear regression (red lines). The DDLS signal demonstrates optically anisotropic, elongated polymer self-assemblies in water-DMF 95-5. The slope (translational diffusion coefficient) is 7.45 ± 0.21 x 10-12 m2/s from DLS, similar to the 7.13 ± 0.96 x 10-12 m2/s, obtained from DDLS. The intercept in DDLS corresponds to the rotational diffusion coefficient (2835.3 ± 352.5 1/s). The corresponding correlation functions are shown in Figure S17.

With clear evidence for solvent-driven folding of our polymers, molecular dynamics simulations were performed to obtain molecular insights into the observed folding in pure DMF and water. Force field parameters for the monomer units were taken from the second generation General Amber Force Field 2 (GAFF2)[37] [20]; atomic charges were computed consistently to the protocol employed for the chosen force field. The structure of each monomer unit was optimized through density functional theory (DFT) calculation *in*

vacuo at B3LYP/6-31G(d,p) level of theory[38,39,40] and the electrostatic potential was subsequently computed starting from the optimized geometries at HF/6-31G* level of theory *in vacuo*. All calculations were carried out with Gaussian09[41] (see supporting information for further details).

Of particular interest was whether the predicted helical folding of the polymers could be followed by simulation. To carry out the simulations, we focused on a polymer chain carrying the hydrophilic side chains linked via esters, such as in **6a**. The model chain was composed of 15 repeat units (thus 30 phenyl rings) identical to those of **6a**. For simulations in the solvent DMF, uncharged tertiary amines were modelled, for simulations in water protonated tertiary amines were modelled (with the chain thus carrying a net positive charge equal to + 15).

After preliminary simulations of the model polymers in both DMF and water (see supporting information) we employed parallel tempering metadynamics in the well-tempered ensemble (PTMetaD-WTE),[42,43] since it combines the advantages of a multi-replica method with metadynamics-based techniques. On the one side, this approach allows obtaining the system's free energy under investigation as a function of a few relevant degrees of freedom (also referred to as collective variables (CV)) by applying a time-dependent bias potential. On the other side, using a multi-replica method can compensate for the limited number of CV that can be directly biased with metadynamics-based schemes thanks to the high-temperature replicas, enhancing the exploration of the conformational space. The well-tempered ensemble allows reducing the needed number of replicas, optimizing the computational effort.

We have chosen two collective variables for the system under investigation: $\pi - \pi$ stacking between the aromatic rings in the polymer (**6a**) backbone and the number of hydrophobic contacts between the aliphatic fragments (*N*-ethylhexyl side chains) of the hydrophobic core of the helix. The first one can discriminate the attainment of unfolded and folded polymer conformations, as well as the presence of an ordered stacking, while the second one is representative of the packing of the ethylhexyl chains in the core.

In essence, high $\pi - \pi$ stacking values (Figures 4 and 5, x-axis) indicate the formation of an ordered stack and high hydrophobic contact values (Figures 4 and 5, y-axis) correspond to an effective packing of the side chains in a hydrophobic core.

The simulated free energy surfaces (FES) and representative polymer structures are shown in Figures 4 and 5. The FES for the polymer in DMF (Figure 4) shows a single relevant energy minimum for low values of both $\pi - \pi$ stacking and hydrophobic contacts, which indicates a lack of ordered stacking and the absence of a hydrophobic core. This clearly shows the preference for an unfolded, fully extended conformation of the polymer chain (Figure 4, I), in agreement with unbiased simulations (Supporting Information) and experimental outcomes. The attainment of a stacked conformation becomes more unfavorable as the stacking order increases, while an effective packing of hydrophobic side chains is essentially absent (Figure 4, II and III).

A different picture is obtained by the conformational sampling of the charged polymer in water. Although the resulting FES still shows a single energy minimum, it is in the region of conformational space representative of ordered stacking and a packed hydrophobic core, according to the chosen collective variables. The sampled conformations show a helical-like arrangement (Figure 5, I) where the hydrophobic segments are in the center of the helix while the charged moieties are exposed to the solvent.

Figure 5 I, furthermore, shows quite nicely how aromatic stacking can be considered an additional driving force for amphiphilic polymers of this type. The roughly ten (stacked) phenyl groups required for one helical turn can readily be counted/visualized in this Figure.

Moreover, the hydrophilic segments are oriented to maximize the distance between charges. A fully extended conformation of the polymer was not observed in the PTMetaD-WTE simulation. The sampled structures characterized by low values of the collective variables (concerning the energy minimum) represent disordered but folded chains (Figure 5, II).

The FES related to the uncharged polymer in water environment (Figure S.29) shows similar features, i.e. the formation of a helical-type structure characterized by ordered $\pi - \pi$ stacking and the presence of a packed hydrophobic core. In this scenario, model outcomes suggest that polymer folding is driven by hydrophobic effects, while the presence of charged moieties is expected to improve solubility and stability in water solutions.

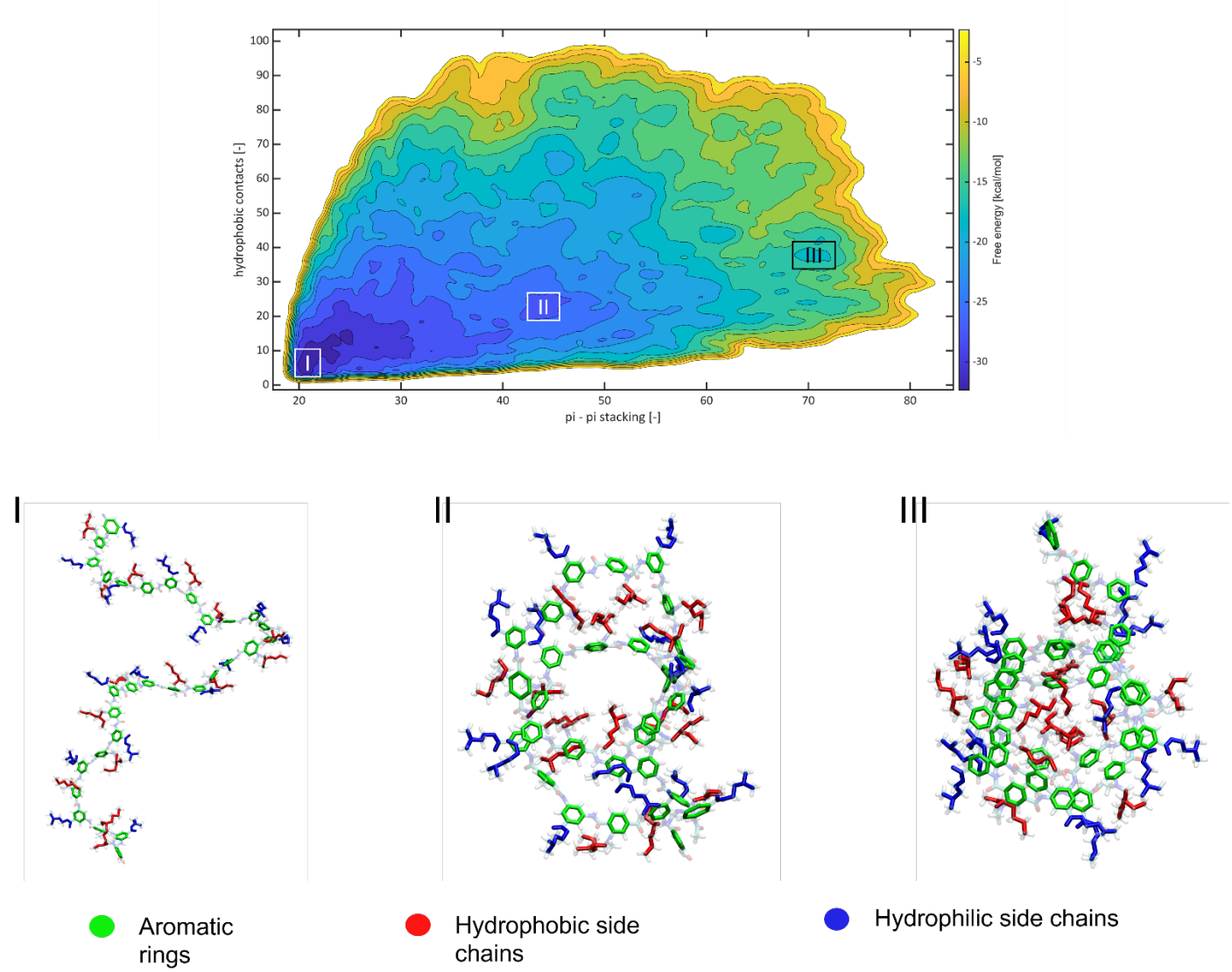

Figure 4 *Top*: Free energy surface as a function of π – π stacking and hydrophobic contacts for uncharged polymer (6a) in DMF along with relevant polymer structures (*top* and *bottom*: I, II, III). Contour lines are plotted every 2 k_BT. Aromatic rings, hydrophobic side chains and hydrophilic side chains are highlighted in green, red and blue, respectively; the overall chain is transparent.

We further extended our analysis by performing 100 ns unbiased MD simulation of a minimum energy conformation in water (see supporting information), using the charged polymer as reference (structure I in Figure 2). The folded arrangement remained stable during the simulation, which allowed us to measure the helix diameter: a single turn is composed of 10 phenyl groups, with an average diameter d = 2.02 ± 0.18 nm. This is in very good agreement with the 2-dimensional drawing in Scheme 2 and in excellent agreement with the experimental data obtained from DDLS.

The simulation results, therefore, strongly support the experimental observations that the amphiphilic polymer **6a-2** adopts a folded structure at high water ratios (as shown by SAXS, see above). Accounting for a hydration layer surrounding the charged helical cylinders, the observed diameter in DDLS (4 nm) is also in excellent agreement with the dimensions calculated from our MD simulations.

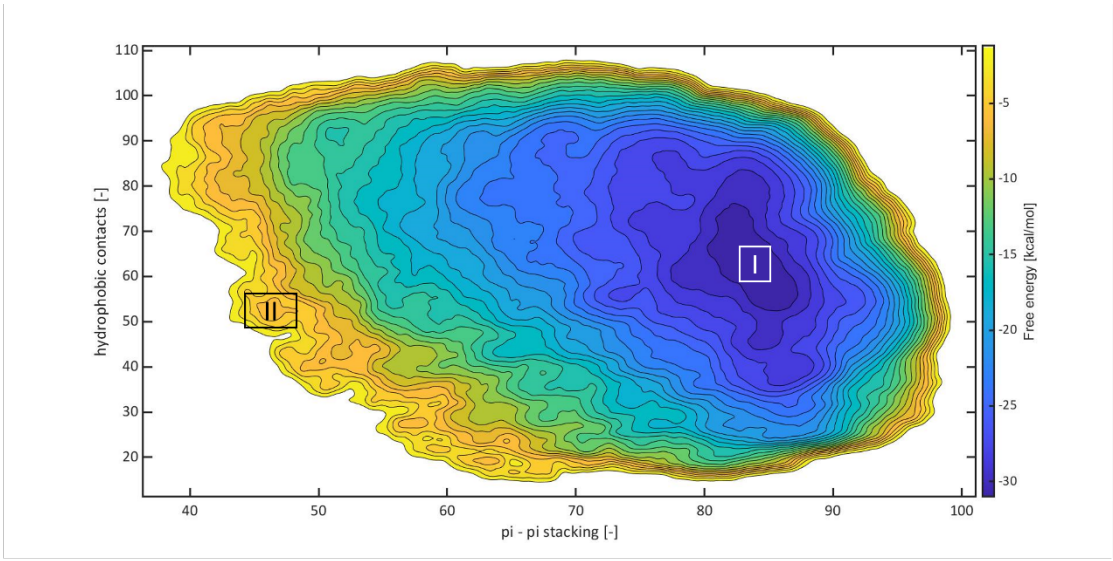

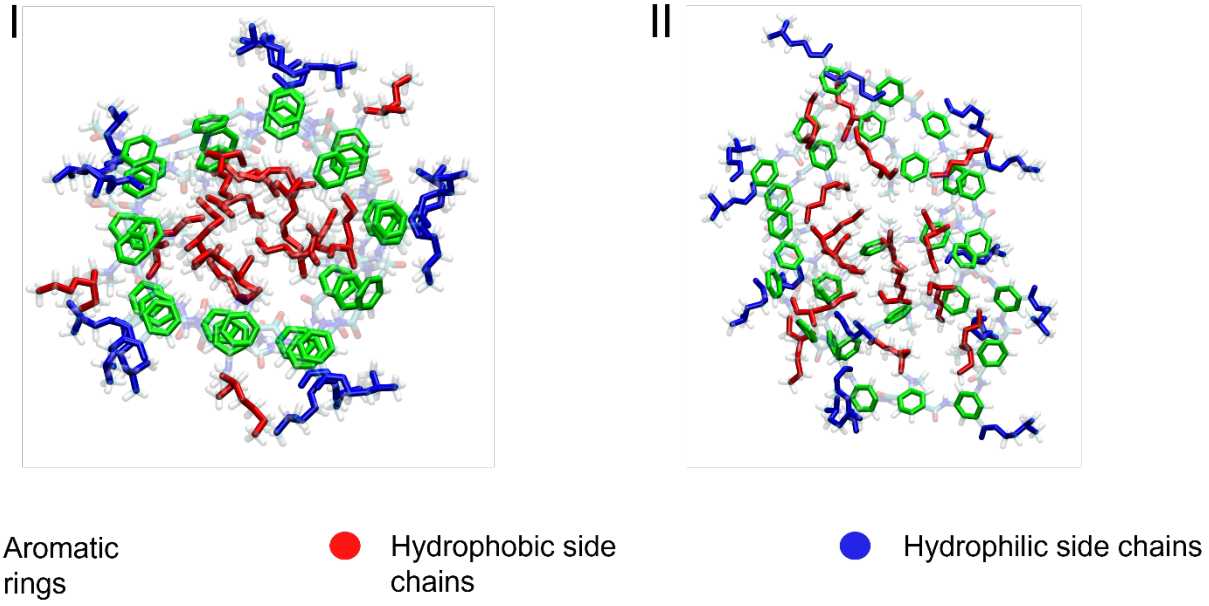

Figure 5 *Top:* Free energy surface as a function of π – π stacking and hydrophobic contacts for charged polymer (6a) in water along with relevant polymer structures (*top* and *bottom*: I, II). Contour lines are plotted every 2 k_BT. Aromatic rings, hydrophobic side chains and hydrophilic side chains are highlighted in green, red, and blue, respectively; the overall chain is transparent.

Conclusion

In conclusion, we have designed and prepared synthetic alternating amphiphilic polymers via step-growth polymerization. These polymers were designed in such a way that upon exposure to highly polar solvents such as water a helical shape should be adopted by the polymer chains. ^{1}H-NMR data and SAXS analysis gave strong indications towards a folded shape in an aqueous environment. AFM analysis of the prepared polymers drop cast from aqueous solutions showed fibre-like structures that further supported the assumed helical folding. Parallel tempering metadynamics simulations gave clear molecular insight into the folded state of the polymers in the two different solvents, DMF and water. We believe that these simulations can be used as very powerful predictive tools to guide the design and synthesis of synthetic foldamers in the future.

ASSOCIATED CONTENT

Supporting Information. Synthetic procedures, UV/vis and NMR spectroscopic data and SAXS data as well as a detailed overview of system parameterization, system preparation and computational protocol is available in Supporting Information. This material is available free of charge via the Internet at http://pubs.acs.org

AUTHOR INFORMATION

Corresponding Authors

Andreas F. M. Kilbinger - Department of Chemistry, University of Fribourg, CH-1700 Fribourg, Switzerland.
orcid.org/0000-0002-2929-7499.
Email: andreas.kilbinger@unifr.ch

Stefan Salentinig - Department of Chemistry, University of Fribourg, CH-1700 Fribourg, Switzerland.
orcid.org/0000-0002-7541-2734.
Email: stefan.salentinig@unifr.ch

Tommaso Casalini†
Department of Chemistry and Applied Bioscience, Institute for Chemical and Bioengineering, ETH Zurich, Vladimir-Prelog-Weg 1-5/10, Zürich, 8093, Switzerland;
Polymer Engineering Laboratory, Institute for Mechanical Engineering and Materials Technology, University of Applied Sciences and Arts of Southern Switzerland (SUPSI), Via la Santa 1, Lugano, 6962, Switzerland.
orcid.org/ 0000-0002-8808-9868.
Email: tommaso.casalini@chem.ethz.ch

Present Addresses

†Oral Product Development, Pharmaceutical Technology and Development, Operations, AstraZeneca, Gothenburg, Pepparedsleden 1, Mölndal 431 83, Sweden

Author Contributions

The manuscript was written through contributions of all authors. / All authors have given approval to the final version of the manuscript. /

ACKNOWLEDGMENTS

AM, SS and AFMK thank the National Center of Competence in Research (NCCR Bio- inspired Materials) and the Fribourg Center for Nanomaterials (FriMat) for support. SD and AFMK thank the Swiss National Science Foundation for funding. TC acknowledges the computational resources provided by ETH Zürich with Euler cluster.

REFERENCES

1 Hamuro, Y. ; Geib, S. J.; Hamilton, A. D. Novel Molecular Scaffolds: Formation of Helical Secondary Structure in a Family of Oligoanthranilamides. *Angew. Chem. Int. Ed.* **1994**, *33*, 446-447.

2 Hamuro, Y. ; Geib, S. J.; Hamilton, A. D. Novel Folding Patterns in a Family of Oligoanthranilamides: Non-Peptide Oligomers That Form Extended Helical Secondary Structure. *J. Am. Chem. Soc.* **1997**, *119*, 10587-10593.

3 Gong, B.; Zeng, H.; Zhu, J.; Yuan, L.; Han, Y.; Cheng, S.; Furukawa, M.; Parra, R. D.; Kovalevsky, A. Y.; Mills, J. L.; Skrzypczak-Jankun, E.; Martinovic, S.; Smith, R. D.; Zheng, C.; Szyperski, T.; Cheng Zeng, X. Creating nanocavities of tunable sizes: Hollow helices. *Proc. Natl. Acad. Sci. U.S.A.* **2002**, *99*, 11583-11588.

4 Gong, B. Hollow Crescents, Helices, and Macrocycles from Enforced Folding and Folding-Assisted Macrocyclization. *Acc. Chem. Res.* **2008**, *41*, 1376-1386.

5 Yuan, L.; Zeng, H.; Yamato, K.; Sanford, A. R.; Feng, W.; Atreya, H. S.; Sukumaran, D. K.; Szyperski, T.; Gong, B. Helical Aromatic Oligoamides: Reliable, Readily Predictable Folding from the Combination of Rigidified Structural Motifs. *J. Am. Chem. Soc.* **2004**, *126*, 16528-16537.

6 Yamato, K.; Kline, M.; Gong, B. Cavity-containing, backbone-rigidified foldamers and macrocyles. *Chem. Commun.* **2012**, *48*, 12142-12158.

7 Zhong, Y.; Kauffmann, B.; Xu, W.; Lu, Z.-L.; Ferrand, Y.; Huc, I.; Zeng, X. C.; Liu, R.; Gong, B. Multiturn Hollow Helices: Synthesis and Folding of Long Aromatic Oligoamides. *Org. Lett.* **2020**, *22*, 6938-6942.

8 Wang, J.; Wicher, B.; Méndez-Ardoy, A.; Li, X.; Pecastaings, G.; Buffeteau, T.; Bassani, D. M.; Maurizot, V.; Huc, I. Loading Linear Arrays of CuII Inside Aromatic Amide Helices. *Angew. Chem. Int. Ed.* **2021**, *60*, 18461-18466.

9 Gillies, E. R.; Dolain, C.; Léger, J.-M.; Huc, I. Amphipathic Helices from Aromatic Amino Acid Oligomers. *J. Org. Chem.* **2006**, 71, 7931-7939.

10 Jiang, H.; Léger, J.-M.; Dolain, C. ; Guionneau, P. ; Huc, I. Aromatic δ-peptides : design, synthesis and structural studies of helical, quinoline-derived oligoamide foldamers. *Tetrahedron* **2003**, *59*, 8365-8374.

11 Dolain, C.; Grélard, A.; Laguerre, M.; Jiang, H.; Maurizot, V.; Huc, I. Solution Structure of Quinoline- and Pyridine-Derived Oligoamide Foldamers. *Chem. Eur. J.* **2005**, *11*, 6135-6144.

12 Li, X.; Markandeya, N.; Jonusauskas, G.; McClenaghan, N. D.; Maurizot, V.; Denisov, S. A.; Huc, I. Photoinduced Electron Transfer and Hole Migration in Nanosized Helical Aromatic Oligoamide Foldamers. *J. Am. Chem. Soc.* **2016**, *138*, 13568-13578.

13 Qi, T.; Deschrijver, T.; Huc, I. Large-scale and chromatography-free synthesis of an octameric quinoline-based aromatic amide helical foldamer. *Nat. Protoc.* **2013**, *8*, 693-695.

14 Li, X.; Qi, T.; Srinivas, K.; Massip, S.; Maurizot, V.; Huc, I. Synthesis and Multibromination of Nanosized Helical Aromatic Amide Foldamers via Segment-Doubling Condensation. *Org. Lett.* **2016**, *18*, 1044-1047.

15 Li, C.; Ren, S.-F.; Hou, J.-L.; Yi, H.-P.; Zhu, S.-Z.; Jiang, X.-K.; Li, Z.-T. F···H-N Hydrogen Bonding Driven Foldamers: Efficient Receptors for Dialkylammonium Ions. *Angew. Chem. Int. Ed.* **2005**, *44*, 5725-5729.

16 Yi, H.-P.; Li, C.; Hou, J.-L.; Jiang, X.-K.; Li, Z.-T. Hydrogen-bonding-induced oligoanthranilamide foldamers. Synthesis, characterization, and complexation for aliphatic ammonium ions. *Tetrahedron* **2005**, *61*, 7974-7980.

17 Urushibara, K.; Masu, Mori, H.; Azumaya, I.; Hirano, T.; Kagechika, H.; Tanatani, A. Synthesis and Conformational Analysis of Alternately *N*-Alkylated Aromatic Amide Oligomers. *J. Org. Chem.* **2018**, *83*, 14338-14349.

18 Cao, R.; Rossdeutcher, R. B.; Wu, X.; Gong, B. Oligo(5-amino-*N*-acylanthranilic acids): Amide Bond Formation without Coupling Reagent and Folding upon Binding Anions. *Org. Lett.* **2020**, *22*, 7496-7501.

19 Zhang, D.-W.; Wang, H.; Li, Z.-T. Polymeric Tubular Aromatic Amide Helices. *Macromol. Rapid Commun.* **2017**, *38*, 1700179.
20 Cao, J.; Kline, M.; Chen, Z.; Luan, B.; Lv, M.; Zhang, W.; Lian, C.; Wang, Q.; Huang, Q.; Wei, X.; Deng, J.; Zhu, J.; Gong, B. Preparation and helical folding of aromatic polyamides. *Chem. Commun.* **2012**, *48*, 11112-11114.
21 Lu, Y.-X.; Shi, Z.-M.; Li, Z.-T.; Guan Z. Helical polymers based on intramolecularly hydrogen-bonded aromatic polyamides. *Chem. Commun.* **2010**, *46*, 9019-9021.
22 Shen, J.; Fan, J.; Ye, R.; Li, N.; Mu, Y.; Zeng, H. Polypyridine-Based Helical Amide Foldamer Channels: Rapid Transport of Water and Protons with High Ion Rejection. *Angew. Chem. Int. Ed.* **2020**, *59*, 13328-13334.
23 Ong, W. Q.; Zhao, H.; Du, Z.; Yeh, J. Z. Y.; Ren, C.; Tan, L. Z. W. ; Zhang K.; Zeng, H. Computational prediction and experimental verification of pyridine-based helical oligoamides containing four repeating units per helical turn, Chem. *Commun.* **2011**, *47*, 6416-6418.
24 Nelson, J. C.; Saven, J. G.; Moore, J. S.; Wolynes, P. G. Solvophobically Driven Folding of Nonbiological Oligomers. *Science* **1997**, *277*, 1793-1796.
25 Stone, M. T.; Moore, J. S. A Water-Soluble m-Phenylene Ethynylene Foldamer. *Org. Lett.* **2004**, *6*, 469-472.
26 Mikami, K.; Yokozawa, T. Helical Folding of Poly(naphthalenecarboxamide) in Apolar Solvent. *J. Polym. Sci., Part A: Polym. Chem.* **2013**, *51*, 739-742.
27 Mikami, K.; Tanatani, A.; Yokoyama, A.; Yokozawa, T. Helical Folding of Poly(naphthalenecarboxamide) Prompted by Solvophobic Effect. *Macromolecules* **2009**, *42*, 3849-3851.
28 Zhang, P.; Zhang, L.; Wang, H.; Zhang, D.-W.; Li, Z.-T. Helical folding of an arylamide polymer in water and organic solvents of varying polarity. *Polym. Chem.* **2015**, *6*, 2955-2961.
29 Zhang, P.; Wang, Z.; Zhang, L.; Wang, H.; Zhang, D.; Hou, J.; Li, Z.-T. Aromatic Amide Polymers that Form Two Helical Conformations with Twist Sense Bias in Water. *Chin. J. Chem.* **2016**, *34*, 678-682.
30 Zhang, P.; Zhang, L.; Wang, Z.-K.; Zhang, Y.-C.; Guo, R.; Wang, H.; Zhang, D.-W.; Li, Z.-T. Guest-Induced Arylamide Polymer Helicity: Twist-Sense Bias and Solvent-Dependent Helicity Inversion. *Chem. Asian J.* **2016**, *11*, 1725-1730.
31 Yamazaki, N.; Higashi, F.; Kawabata, J. Studies on Reactions of the *N*-Phosphonium Salts of Pyridines. XI Preparation of Polypeptides and Polyamides by Means of Triaryl Phosphites in Pyridine. *J. Polym. Sci. Pol. Chem.* **1974**, *12*, 2149-2154.
32 Yamazaki, N.; Higashi, F. Studies on Reactions of the N-Phosphonium Salts of Pyridines – VII Preparation of Peptides and Active Esters of Amino Acids using Diphenyl and Triphenyl Phosphites in the Presence of Tertiary Amines. *Tetrahedron* **1974**, *30*, 1323-1326.
33 Hamborg, E. S., Versteeg, G.F. Dissociation Constants and Thermodynamic Properties of Amines andAlkanolamines from (293 to 353) K. *J. Chem. Eng. Data.* **2009**, *54*, 1318-1328.
34 Guo, R.; Zhang, L.; Wang, H.; Zhang, D.-W.; Li, Z.-T. Hydrophobically driven twist sense bias of hollow helical foldamers of aromatic hydrazide polymers in water. *Polym. Chem.* **2015**, *6*, 2382-2385.
35 Itoh, Y.; Chen, S.; Hirahara, R.; Konda, T.; Aoki, T.; Ueda, T.; Shimada, I.; Cannon, J.; Shao, C.; Aida, T. Ultrafast water permeation through nanochannels with a densely fluorous interior surface. *Science* **2022**, *376*, 738-743.
36 Vazquez-Gonzalez, V.; Mayoral, M.J.; Aparicio, F.; Martinez-Arjona, P.; Gonzalez-Rodriguez, D. The Role of Peripheral Amide Groups as Hydrogen-Bonding Directors in the Tubular Self-Assembly of Dinucleobase Monomers. *ChemPlusChem* **2021**, *86*, 1087-1096.
37 Wang, J. M.; Wolf, R. M.; Caldwell, J. W.; Kollman, P. A.; Case, D. A. Development and testing of a general amber force field. *J. Comput. Chem.* **2004**, *25*, 1157-1174.
38 Becke, A. D., Density-Functional Thermochemistry .3. The Role of Exact Exchange. *J. Chem. Phys.* **1993**, *98*, 5648-5652.
39 Lee, C. T.; Yang, W. T.; Parr, R. G. Development of the Colle-Salvetti Correlation-Energy Formula into a Functional of the Electron-Density. *Phys. Rev. B* **1988**, *37*, 785-789.
40 Ditchfield, R.; Hehre, W. J.; Pople, J. A., Self-Consistent Molecular-Orbital Methods .9. Extended Gaussian-Type Basis for Molecular-Orbital Studies of Organic Molecules. *J. Chem. Phys.* **1971**, *54*, 724-728.
41 Frisch, M. J.; Trucks, G. W.; Schlegel, H. B.; Scuseria, G. E.; Robb, M. A.; Cheeseman, J. R.; Scalmani, G.; Barone, V.; Petersson, G. A.; Nakatsuji, H.; Li, X.; Caricato, M.; Marenich, A. V.; Bloino, J.; Janesko, B. G.; Gomperts, R.; Mennucci, B.; Hratchian, H. P.; Ortiz, J. V.; Izmaylov, A. F.; Sonnenberg, J. L.; Williams; Ding, F.; Lipparini, F.; Egidi, F.; Goings, J.; Peng, B.; Petrone, A.; Henderson, T.; Ranasinghe, D.; Zakrzewski, V. G.; Gao, J.; Rega, N.; Zheng, G.; Liang, W.; Hada, M.; Ehara, M.; Toyota, K.; Fukuda, R.; Hasegawa, J.; Ishida, M.; Nakajima, T.; Honda, Y.; Kitao, O.; Nakai, H.; Vreven, T.; Throssell, K.; Montgomery Jr., J. A.; Peralta, J. E.; Ogliaro, F.; Bearpark, M. J.; Heyd, J. J.; Brothers, E. N.; Kudin, K. N.; Staroverov, V. N.; Keith, T. A.; Kobayashi, R.; Normand, J.; Raghavachari, K.; Rendell, A. P.; Burant, J. C.; Iyengar, S. S.; Tomasi, J.; Cossi, M.; Millam, J. M.; Klene, M.; Adamo, C.; Cammi, R.; Ochterski, J. W.; Martin, R. L.; Morokuma, K.; Farkas, O.; Foresman, J. B.; Fox, D. J. Gaussian 09 Rev. D.01, Wallingford, CT, 2016.
42 Deighan, M.; Bonomi, M.; Pfaendtner, J. Efficient Simulation of Explicitly Solvated Proteins in the Well-Tempered Ensemble. *J. Chem. Theory Comput.* **2012**, *8*, 2189-2192.
43 Bonomi, M.; Parrinello, M. Enhanced Sampling in the Well-Tempered Ensemble. *Phys. Rev. Lett.* **2010**, *104*, 190601.

graphical abstract